Multi-band Cosmology Using Centi-Hertz Gravitational Wave Sources

Rhondale Tso[1,2,*]

[1] *DARK, Niels Bohr Institute, University of Copenhagen, Blegdamsvej 17, 2100 Copenhagen, Denmark*

[2] *TAPIR 350-17, California Institute of Technology, 1200 E California Boulevard, Pasadena, CA 91125, USA*

(Dated: September 30, 2017)

Abstract

As Adv. LIGO completes its second observation run, the expectation of further gravitational wave (GW) events and space-based LISA detectors in the near future provide the promise of further exploration of GW150914-like signals across multiple bands. Future, third-generation detectors are expected to improve sensitivities and allow GW observations from the decihertz to kilohertz range. Along with the added sensitivities and sky-localization, the multi-band observation adds the promise of mapping weak lensing potentials and enhancing GW cosmology. This report describes the progress on this research program that has been made so far.

* rtso@caltech.edu

I. INTRODUCTION

Direct detections of gravitational waves (GWs) by the LIGO Scientific Collaboration [1–5] are historic and have also provided interesting prospects of multi-band GW astronomy since some of the systems observed by LIGO to date would also have been observable by a space-based Laser Interferometer Space Antenna (LISA) [6]. Given space-based detectors, observing in conjunction with Adv. LIGO, GW150914-like systems will be detectable in the cHz range, merging in Adv. LIGO's band on a timescale of less than a decade [6]. Multi-band GW observations have the potential to shed light on the BH-formation mechanisms [7] and constrain dipole emission of GWs [8].

In December of 2015, the European Space Agency launched *LISA Pathfinder*, a technology demonstration mission that has been a great success [9]. The results have also provided updated noise curves for a new LISA design set to launch in the next 20 years [10]. One of the science objectives for LISA is to keep a GW150914-like system detectable in the LISA band with a (signal-to-noise) SNR threshold $\rho_{\rm LISA} \geq 7$ during the four year space mission. This would advance GW astronomy to begin observing GW signals across multiple bandwidths. Once a GW150914-like system advances to 1 decihertz, the signal will enter Adv. LIGO's band on a timescale of two weeks. This advance warning allows electromagnetic observers to concentrate on the source's sky location for any (although rare) EM counterpart and perform additional tests of GR.

One major advantage to multi-band observations is the accurate sky-localization, which, along with an identified host galaxy [11], will give an independent measurement of the luminosity distance and redshift. This will also allow accurate study of GW cosmology and the possibility of studying weak-lensing potentials. At cosmological distances every GW source will be gravitationally lensed, causing a magnification or demagnification of the observed shear signal at the detector. The presence of this signal can be inferred statistically. Ref. [12] analyzed precision measurements of fundamental cosmological parameters, including measuring the gravitational-lensing convergence power spectrum, in which errors on the absolute luminosity distance is dominated by effects of gravitational lensing magnification. Here the power spectrum from weak lensing shear is not only sensitive to distances between the observer, lens, and source, but also to the distribution of lenses. Measuring this distribution of lens and mapping the weak lensing potential will provide insight to growth of density

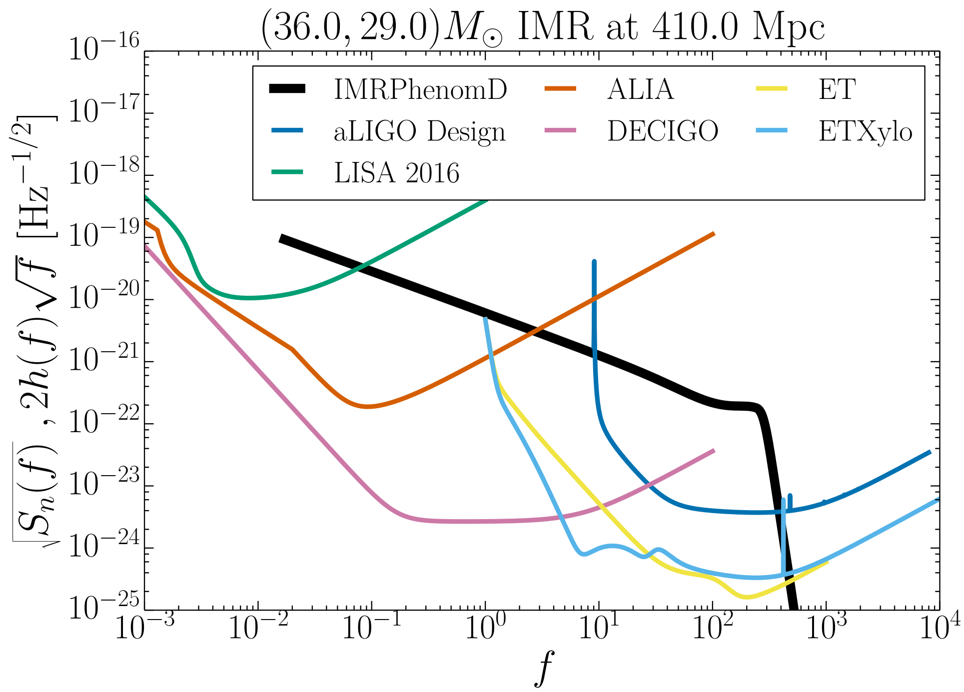

FIG. 1. GW strain of a GW150914-like event extended to the cHz range. Along with the strain are current and future detectors. From 1.7 cHz, the signal is expected to coalesce in 4.03 years with $\rho_{\rm LISA} = 7$ and $\rho_{\rm LIGO} = 97$.

perturbations. The primary analysis of Ref. [12] relied on a future space-based mission: *Big Bang Observer*. Our work aims to extend the mapping of weak lensing potentials utilizing detectors attainable in the near future: LISA, Adv. LIGO, Einstein Telescope (ET), Deci-hertz Interferometer Gravitational wave Observatory (DECIGO), and Advanced Laser Interferometer Antenna (ALIA). Here the primary analysis focuses on the next two decades of observers: LISA and Adv. LIGO.

To begin a study of weak lensing potentials through GWs, the estimated number of binaries observable in both bands needs to be assessed. This report summarizes the rates at which events are expected to occur to accomplish multi-band GW cosmology using most recent rate estimates [3] and techniques utilized in Ref. [13].

A. Multi-Band GW Astronomy

During the early inspiral of binary black holes (BBHs) Keplerian motion can, to zeroth order, be used to describe their motion and come to a description of the leading order evolution of the binary due to GW emission [14]. Given two component masses $m_{1,2}$, the total mass and symmetric mass ratio are $M = m_1 + m_2$ and $\eta = m_1 m_2/M^2$, respectively. Here the orbital period P of the binary is related to the semi-major axis a as $P^2 \propto a^3$. The dominant GW frequency f is twice the orbital frequency of the binary, thus we can say $a \propto f^{-2/3}$. Ref. [14] provides a description of the time evolution of a circular binary due to GW emission, inspiraling and coalescing on a timescale $T_c(a) \propto a^4$. Between two frequencies $f_{\rm low}$ and $f_{\rm up}$ this explicitly comes out as,

$$T = \frac{5}{256\eta}\frac{GM}{c^3}\left(\left(\frac{GM}{c^3}\pi f_{\rm low}\right)^{-8/3} - \left(\frac{GM}{c^3}\pi f_{\rm up}\right)^{-8/3}\right) \tag{1}$$

In this interval, the SNR accumulated is expressed as,

$$\rho = 4\Re\int_{f_{\rm low}}^{f_{\rm up}} df\, \frac{h(f)^* h(f)}{S_n(f)} \tag{2}$$

where $h(f)$ is a frequency dependent GW strain and $S_n(f)$ is the noise curve associated with the detector. For example, all detections with Adv. LIGO have had T_c varying from less than a second to a little under two seconds while accumulating an $\rho \sim 10 - 30$ at O1/O2 sensitivities. The most massive, GW150914, would have advanced from 1.7 cHz to 10 cHz in 4 years with a LISA SNR of 7.

The full inspiral-merger-ringdown waveform [1], from the early inspiral to coalescence, of a GW150914-like system is plotted in figure 1, alongside noise curves of Adv. LIGO, LISA, and third generation detectors. Here $\rho_{\rm LISA} = 7$ and at design $\rho_{\rm LIGO} = 97$. Although future detectors, e.g., ALIA, ET, etc., will all have tremendously improved sensitivities, we concentrate on detectors expected to come online within the next two decades. Here the lower frequency of the IMR waveform is set so that $f_{\rm up} = 1$ dHz when calculating $\rho_{\rm LISA}$. The observing time is then set to LISA's space mission of $T = 4$ years. Then, using (1) we can estimate what the lower frequency is, which comes out to 1.7 cHz for a $(36, 29)M_\odot$ system. The total time to coalesce from 1.7 cHz is 4.03 years. This exemplifies the type of

[1] Using IMRPhenomD.

system expected to be observed in both bands. More massive systems will have lower $f_{\rm low}$ when $f_{\rm up} = 1$ dHz and $T = 4$ years are fixed, allowing more SNR to be accumulated while still merging on a time scale of ~ 4 years.

B. Rates Estimation

Provided an overall rate density, R, for the number of BBH mergers $\mathrm{yr}^{-1}\mathrm{Gpc}^{-3}$, from some model, we assume a probability density for the intrinsic masses of the black hole binaries in the population. The probability densities are a log-uniform distribution $p \propto m_1^{-1} m_1^{-2}$ and a power-law (Salpeter) distribution $p \propto m_1^{-\alpha}$, which is uniform in m_2. Currently $\alpha = 2.35$. Here m_1 is treated as the primary with $m_1 \in (m_{\rm min}, m_{\rm max})$ and $m_2 \in (m_{\rm min}, m_1)$ where $m_{\rm min} = 5M_\odot$ and $m_1 + m_2 \leq 100M_\odot$. The rate density R is take as the median estimated rates based on the current set of LIGO events and population models consistent with the log-uniform distribution, $R = 30\ \mathrm{yr}^{-1}\mathrm{Gpc}^{-3}$, and the power-law distribution, $R = 100\ \mathrm{yr}^{-1}\mathrm{Gpc}^{-3}$ [3].

The total number N of BBHs expected to be observed per year by any given detector is calculated with,

$$N = \int\limits_{m_{\rm min}}^{m_{\rm max}} \int\limits_{m_{\rm min}}^{m_1} \int R\tilde{V}_c p \, dm_2 dm_1 \tag{3}$$

in which we take an observer time-weighted co-moving volume within which a source of intrinsic masses can be observed,

$$\tilde{V}_c(m_1, m_2) = \int\limits_0^{z_{\rm max}(m_1,m_2)} dz \, \frac{1}{(1+z)} \frac{dV_c}{dz} \tag{4}$$

Above, a cosmology is specified, characterized by the resulting differential co-moving volume density, dV_c/dz. Here $\tilde{V}_c$ depends on the maximal redshift that a source can be seen given intrinsic masses (m_1, m_2), set by an SNR threshold, which is set to $\rho_{\rm th} = 8$ for Adv. LIGO. Methods to calculate $z_{\rm max}(m_1, m_2)$ involve: 1) a method of bisection that iteratively solves for $z_{\rm max}$ for each (m_1, m_2) in our grid, or 2) working with redshifted masses, then performing a coordinate transformation to get $\tilde{V}_c(m_1, m_2)$. Choosing the former, the result $d\tilde{V}_c$ is then integrated to $z_{\rm max}$ while being weighted by the antenna-weight power distribution plotted in the left panel of figure 2. Summing over this weighting factor is equivalent to taking into

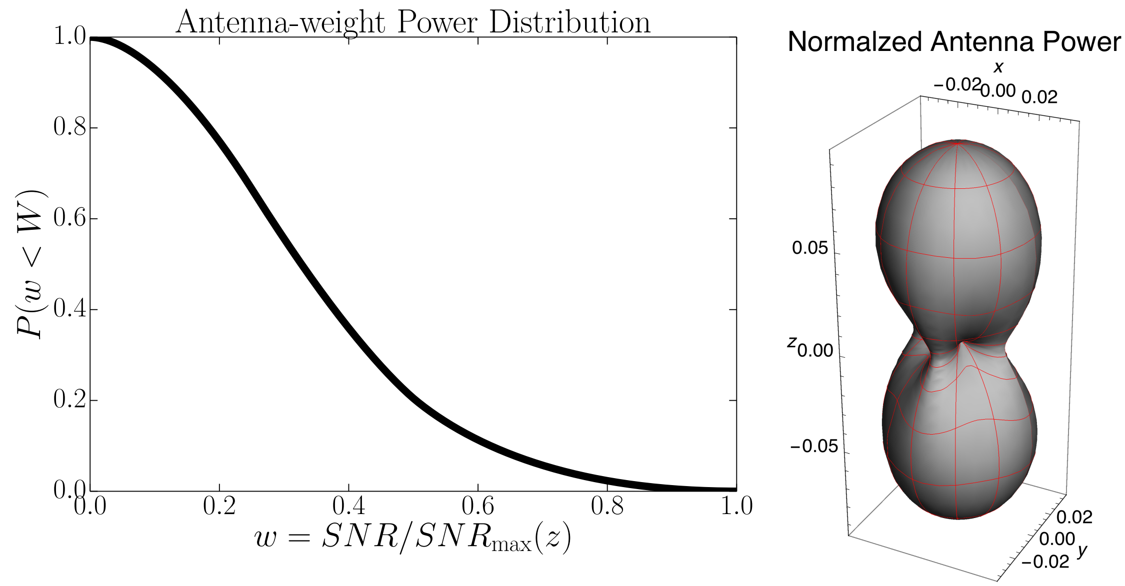

FIG. 2. Left: Antenna-weight power distribution implemented in integrating (4). This is equivalent to weighing the horizon distance by a "peanut" factor of 1/2.26. Right: Antenna power distribution of a single detector. MCMC methods evaluate a 1/2.26 weight factor.

account the antenna "peanut" factor 1/2.26 often calculated via MCMC methods, e.g., see antenna power for single Adv. LIGO detector in right panel of figure 2.

II. RESULTS

Assuming Adv. LIGO at design, we calculate $z_{\max}, \tilde{V}_c$, and N over a grid of masses set by $m_1 \in (m_{\min}, m_{\max})$ and $m_2 \in (m_{\min}, m_1)$ with $m_{\min} = 5M_\odot$ and $m_1 + m_2 \leq 100M_\odot$. The mass spacing in this grid is set to $0.5M_\odot$. In the top left panel of figure 3, the maximal redshift $z_{\max}$ for each set of masses is calculated via an iterative process by specifying component masses $m_{1,2}$ and method of bisection. Next $\tilde{V}_c$ is calculated after weighted by the antenna-weight power distribution displayed in figure 2. Using these primary ingredients we then use normalized probability densities p for the masses of the BBH in the population. In this analysis we use a log-uniform distribution $p \propto m_1^{-1} m_1^{-2}$ and a power-law (Salpeter) distribution $p \propto m_1^{-2.35}$, which is uniform in m_2. The results for the log-uniform distribution are displayed in the bottom left panel of figure 3 and the power-law distribution results are the bottom right panel of figure 3.

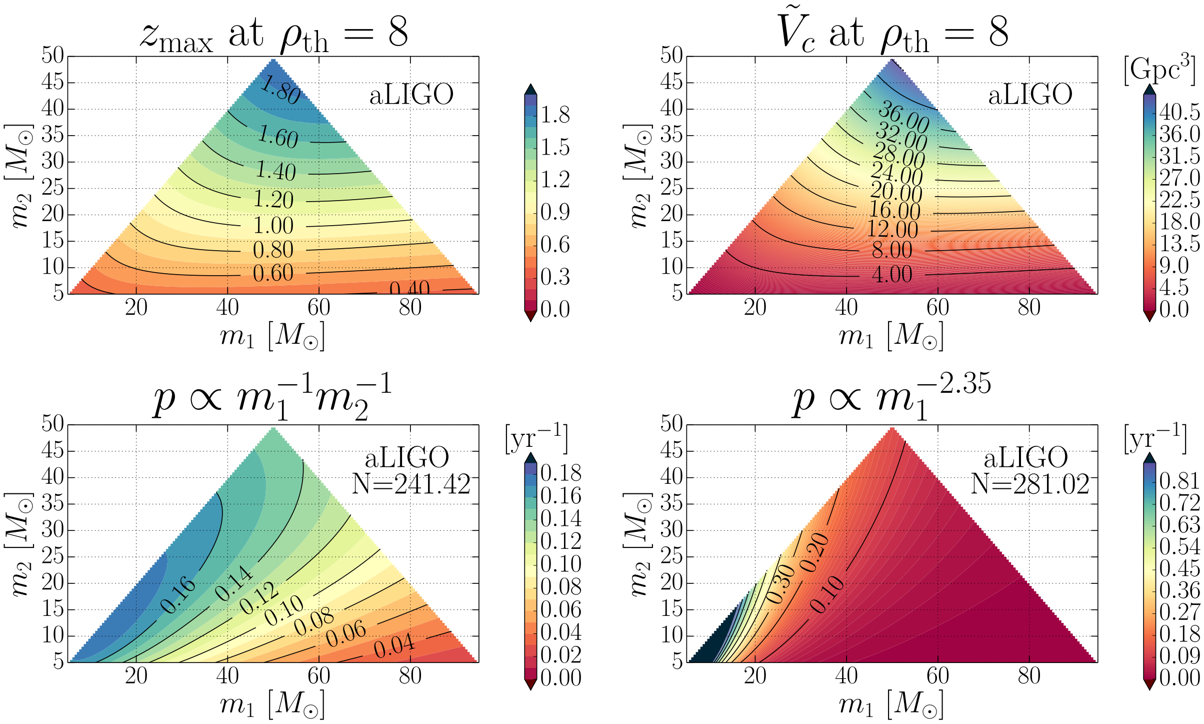

FIG. 3. Top Left: Maximal redshift evaluated via an iterative method of bisection for each pair of component masses $m_{1,2}$ on the mass grid. Top Right: Time-weighted co-moving volume as a function of $m_{1,2}$. Bottom Left: Distribution of N over the mass grid for the log-uniform distribution. Bottom Right: Distribution of N over the mass grid for the power-law distribution. All grid spacings are set by $0.5M_\odot$ and total N for each mass distribution are displayed. Adv. LIGO design noise curves are assumed and evaluated with IMRPhenomD.

Summing all over mass bins we get $N = 241$, for the log-uniform, and $N = 281$, for the power-law. We can also perform partial sums, where for the log-uniform we get the following rates in the specified mass ranges,

$$N = 1.9, m_1 \in (5, 10)M_\odot$$

$$N = 92.5, m_1 \in (5, 40)M_\odot$$

$$N = 148.9, m_1 \in (40, 100)M_\odot$$

and for the power-law,

$$N = 57.5, m_1 \in (5, 10)M_\odot$$

$$N = 221.0, m_1 \in (5, 40)M_\odot$$

$$N = 60.0, m_1 \in (40, 100)M_\odot$$

For a LISA analysis on N, some caveats exist. To perform the analysis for LISA the SNR accumulated is restricted by the space missions duration (4 years). We need to accumulate the SNR over the full observation time so conversion between number of events with SNR above a threshold and the rate is not just a case of multiplying by the mission duration. Given that the signals duration is much longer than the detector's relative orientation during observation, the antenna-weight power distribution also needs to be reevaluated. Such efforts are currently in the works.

III. FUTURE WORK

Provided a sample of N binaries detectable by joint LISA-LIGO observations, the study of weak lensing potentials with GW observations will provide insight on growth of density perturbations and tests of GR. Extending this study to ALIA, ET, and DECIGO, a full analysis of multi-band GW cosmology with future detectors will be performed.

ACKNOWLEDGMENTS

This work was performed at the Niels Bohr Institute under the supervision of Jonathan Gair, Daniel E. Holz, and Joey S. Key. We thank the Niels Bohr Institute for its hospitality while part of this work was completed, and acknowledge the Kavli Foundation and the DNRF for supporting the 2017 Kavli Summer Program.

[1] B. P. Abbott *et al.* (LIGO and Virgo Scientific Collaboration), PRL **116**, 061102 (2016), arXiv:1602.03837 [gr-qc].

[2] B. P. Abbott *et al.* (LIGO and Virgo Scientific Collaboration), PRL **116**, 241103 (2016), arXiv:1606.04855 [gr-qc].

[3] B. P. Abbott *et al.*, PRX **6** (2016), 10.1103/PhysRevX.6.041015.

[4] B. P. Abbott *et al.* (LIGO and Virgo Scientific Collaboration), PRL **118**, 221101 (2017), arXiv:1706.01812 [gr-qc].

[5] B. P. Abbott *et al.*, LIGO-P170814 (2017).

[6] A. Sesana, PRL **116**, 231102 (2016), arXiv:1602.06951 [gr-qc].

[7] A. Nishizawa, E. Berti, A. Klein, and A. Sesana, PRD **94**, 064020 (2016), arXiv:1605.01341 [gr-qc].

[8] E. Barausse, N. Yunes, and K. Chamberlain, PRL **116**, 241104 (2016), arXiv:1603.04075 [gr-qc].

[9] M. Armano *et al.*, PRL **116** (2016), 10.1103/PhysRevLett.116.231101.

[10] P. Amaro-Seoane *et al.* (LISA Core Team), ArXiv e-prints (2017), arXiv:1702.00786 [astro-ph.IM].

[11] H. Chen and D. Holz, ArXiv e-prints (2016), arXiv:1612.01471 [astro-ph.HE].

[12] C. Cutler and D. Holz, PRD **80** (2009), 10.1103/PhysRevD.80.104009.

[13] H. Chen, D. Holz, J. Miller, E. Evans, S. Vitale, and J. Creighton, ArXiv e-prints (2017), arXiv:1709.08079 [astro-ph.CO].

[14] P. Peters, PRD **136** (1964).